ADVANCES IN ATMOSPHERIC SCIENCES, VOL. 26, NO. 4, 2009, 666–678

On the Association between Spring Arctic Sea Ice Concentration and Chinese Summer Rainfall: A Further Study

WU Bingyi*[1] (武炳义), ZHANG Renhe[1] (张人禾), and Bin WANG[2]

[1] *Chinese Academy of Meteorological Sciences, Beijing* 100081

[2] *Department of Meteorology and International Pacific Research Center, University of Hawaii at Manoa, Honolulu, Hawaii*

(Received 23 January 2009; revised 10 March 2009)

ABSTRACT

In our previous study, a statistical linkage between the spring Arctic sea ice concentration (SIC) and the succeeding Chinese summer rainfall during the period 1968–2005 was identified. This linkage is demonstrated by the leading singular value decomposition (SVD) that accounts for 19% of the co-variance. Both spring SIC and Chinese summer rainfall exhibit a coherent interannual variability and two apparent interdecadal variations that occurred in the late 1970s and the early 1990s. The combined impacts of both spring Arctic SIC and Eurasian snow cover on the summer Eurasian wave train may explain their statistical linkage. In this study, we show that evolution of atmospheric circulation anomalies from spring to summer, to a great extent, may explain the spatial distribution of spring and summer Arctic SIC anomalies, and is dynamically consistent with Chinese summer rainfall anomalies in recent decades. The association between spring Arctic SIC and Chinese summer rainfall on interannual time scales is more important relative to interdecadal time scales. The summer Arctic dipole anomaly may serve as the bridge linking the spring Arctic SIC and Chinese summer rainfall, and their coherent interdecadal variations may reflect the feedback of spring SIC variability on the atmosphere. The summer Arctic dipole anomaly shows a closer relationship with the Chinese summer rainfall relative to the Arctic Oscillation.

Key words: spring Arctic sea ice concentration, summer rainfall, Arctic dipole anomaly, interannual and interdecadal variations

Citation: Wu, B. Y., R. H. Zhang, and B. Wang, 2009: On the association between spring arctic sea ice concentration and Chinese summer rainfall: A further study. *Adv. Atmos. Sci.*, **26**(4), 666–678, doi: 10.1007/s00376-009-9009-3.

1. Introduction

It has been recognized that many factors (external forcing and atmospheric circulation pattern) influence the Chinese summer rainfall. Many previous studies have attributed the Chinese summer rainfall variations to ENSO and SST variations in the Pacific and Indian Oceans (Ju and Slingo, 1995; Hu, 1997; Zhang et al., 1996, 1999; Weng et al., 1999; Wang et al., 2000; Chang et al., 20000; Yang and Lau, 2004; Wang and Li, 2004; Li and Wang, 2005). The monsoon-warm ocean interaction is one of the factors that determine the East Asian summer monsoon (EASM) anomalies rather than the SST anomalies in the Indian Ocean and western Pacific (Wang et al., 2003), because the SST anomalies in the Indian Ocean and the western Pacific are largely a result of the atmospheric forcing (Wang et al., 2004; Wang et al., 2005).

Although the influence of SSTs and ENSO events on summer rainfall in China has been recognized, not all the variances of summer rainfall can be explained by the SSTs (Ding et al., 2007). Eurasian snow cover variations and its association with the Asian summer rainfall also have been extensively explored both in observations and simulations, particularly in the relationship with the Indian summer monsoon rainfall (e.g., Wu and Kirtman, 2007). In China, researchers pay more attention to the Tibetan Plateau snow cover

*Corresponding author: WU Bingyi, wby@cams.cma.gov.cn

variability and its association with rainfall in China. In fact, a moderate positive correlation between the Tibetan Plateau snow cover and spring rainfall in southern China contains ENSO's effects, and ENSO has larger impacts than the Tibetan Plateau snow cover on spring rainfall in southern China (Wu and Kirtman, 2007). Yang and Xu (1994) revealed that the Eurasian winter snow cover is positively correlated with the following summer rainfall in northern and southern China and negatively in central, northeast, and western China. Using different snow cover datasets, Wu and Kirtman (2007) investigated the relationship between spring and summer rainfall in East Asia and the preceding winter and spring Eurasian snow cover, and found that spring rainfall variations in southern China are positively correlated with anomalous spring snow cover in western Siberia, whereas the summer rainfall correlations with the spring Eurasian snow cover are weak. Wu et al. (2009a) revealed the first two dominant patterns of spring Eurasian snow water equivalent (SWE) variability and their associations with Chinese summer rainfall during the period of 1979–2004. Their results showed that in the recent two decades, coherent decreased spring SWE in Eurasia may be one of the reasons for severe droughts in north and northeast China and much more significant rainfall events in south and southeast China. A possible physical explanation is that decreased spring SWE in Eurasia strengthened the positive 500 hPa height anomalies over East Asia south of Lake Baikal during the following summer season, leading to the Chinese summer rainfall anomalies. Another dominant pattern of spring SWE variability shows opposite variations in western and eastern Eurasia, and is significantly correlated with the summer rainfall in north and northeast China, that is, less spring SWE in western Eurasia and excessive SWE in eastern Eurasia and the Tibetan Plateau tends to be associated with decreased summer rainfall in north and northeast China.

The role of Arctic sea ice variability in the climate system has been extensively investigated using observations and simulations (Walsh, 1983; Honda et al., 1996; Rigor et al., 2002; Alexander et al., 2004; Deser et al., 2004; Magnusdottir et al., 2004; Wu et al., 2004, 2006; and others). Sea ice variation in the Greenland Sea is closely related to sea ice and freshwater output of the Arctic Ocean (Aagaard and Carmack, 1989; Vinje, 2001; Wu et al., 2006; Wu and Johnson, 2007), with its links to the North Atlantic deep water variation (Lenderink and Haarsma, 1996), the thermohaline circulation adjustment (Mauritzen and Häkkinen, 1997), and interdecadal climate variability (Lazier, 1988; Deser and Blackmon, 1993; Mysak and Venegas, 1998). Coherent interdecadal variability in the atmosphere-ocean-ice system in the Arctic and the North Atlantic requires that sea ice anomalies have an important impact on the atmosphere (Mysak et al., 1990; Mysak and Venegas, 1998).

The feedback of sea ice anomalies on the atmosphere can be roughly divided into the local and large-scale responses. The local response to sea ice anomalies over the subpolar seas of both the Atlantic and Pacific is robust and generally shallow. Where sea ice has receded, atmospheric anomalies are characterized by upward surface heat fluxes, near-surface warming, enhanced precipitation, and below normal sea level pressure (SLP); the reverse is true where sea ice has expanded (Alexander et al., 2004; Wu et al., 2004). Sea ice variation in the Nordic and Barents Seas influences stratification and the stability of the planetary boundary layer, and create the potential for dynamical influences on the atmospheric boundary layer through vertical motion induced by the pressure anomalies in the boundary layer (Wu et al., 2004). The large-scale response to reduced (enhanced) winter sea ice extent to the east (west) of Greenland resembles the negative phase of the Arctic Oscillation (AO) or the North Atlantic Oscillation (NAO) (Alexander et al., 2004). The large-scale response depends on the interaction between the anomalous surface fluxes and the large-scale circulation (Alexander et al., 2004; Deser et al., 2004). Magnusdottir et al. (2004) investigated the atmospheric responses to a realistic spatial pattern of anomalous SST and sea ice forcing (the recent 40-yr trend in SST and sea ice) with an exaggerated anomaly amplitude in the North Atlantic sector. They found that the atmospheric response to the SST anomalies are quite weak compared to the observed positive trend in the NAO, and sea ice extent anomalies are more efficient than SST anomalies in exiting an atmospheric response comparable in amplitude to the observed NAO trend. In reality, it is very difficult to directly detect the feedback of sea ice on the atmosphere because of the dominance of atmospheric forcing of sea ice in the observed association.

There are fewer observational studies on the relationship between the Arctic sea ice and summer rainfall in China (Niu et al., 2003; Zhao et al., 2004). They showed that reduced spring (or the late winter to the early spring) sea ice extent in the Bering and Okhotsk Seas corresponds to an enhanced June-July rainfall in southeast China (Niu et al., 2003; Zhao et al., 2004). However, spring sea ice variability is generally out of phase between the Bering and Okhotsk Seas, thus taking them together is inappropriate (Cavalieri and Parkinson, 1987; Fang and Wallace, 1994).

In our previous study, we revealed a statistical linkage between the spring Arctic sea ice concentration

(SIC) and the Chinese summer rainfall using the singular value decomposition (SVD) method (Wu et al., 2009b). Both the spring SIC and Chinese summer rainfall exhibit a coherent interannual variability and two apparent interdecadal variations that occurred in the late 1970s and the early 1990s. We indicated that the combined impacts of both spring Arctic SIC and Eurasian snow cover on the summer Eurasian wave train may explain their statistical linkage. However, some important issues remain unclear. For example, what mechanism is responsible for the persistent SIC anomalies from spring to summer? What are the features of the evolution of the anomaly in the atmospheric circulation from spring to summer? Additionally, the variations of spring Arctic SIC and Chinese summer rainfall all include clearly both interannual and interdecadal time scales, which time scale contributes more to the identified association? What are the features of the summer circulation anomalies associated with the spring Arctic SIC on interannual and interdecadal time scales, respectively? Apparently, these issues cannot be addressed in a 4-page paper. In the present study, besides answering these issues another possible mechanism is proposed to explain the statistical linkage between the spring Arctic SIC and the Chinese summer rainfall.

2. Data and methods

The primary datasets used in this study are the monthly mean SLP, surface air temperature (SAT) and geopotential heights at 500 hPa obtained from the National Center for Environmental Prediction (NCEP) and the National Center for Atmospheric Research (NCAR) reanalysis datasets for the period of 1968–2007. This period was chosen due to the uncertainties in the reanalysis dataset over East Asia prior to 1968 (Yang et al., 2002). The monthly mean Arctic SIC dataset (on a 1° × 1° grid for the period 1961–2007) was obtained from the British Atmospheric Data Centre (BADC, http://badc.nerc.ac.uk/data/hadisst/). A monthly 513-station rainfall dataset in China was obtained from the National Meteorological Information Centre of China, spanning the period from 1968 to 2005. We also used the gridded monthly sea ice motion data during the periods from 1979 to 2004, taken from ftp://iabp.apl.washington.edu/pub/IABP/D/D784/, to investigate the response of sea ice motion to atmospheric forcing. This study also used the monthly mean AO index during the period 1968–2005 (http://www.cpc.noaa.gov/products/precip/CWlink/daily_ao_index/) to explore its association with summer rainfall variability in China.

In this study, the empirical orthogonal function (EOF) analysis is applied to the summer mean SLP north of 70°N to extract the summer dipole anomaly. We focus on the seasonal means, averaged for three spring (March–May) and summer (June–August) months.

3. Evolution of anomalies in Arctic SIC and atmospheric circulation from spring to summer

Figure 1 shows the time series and corresponding

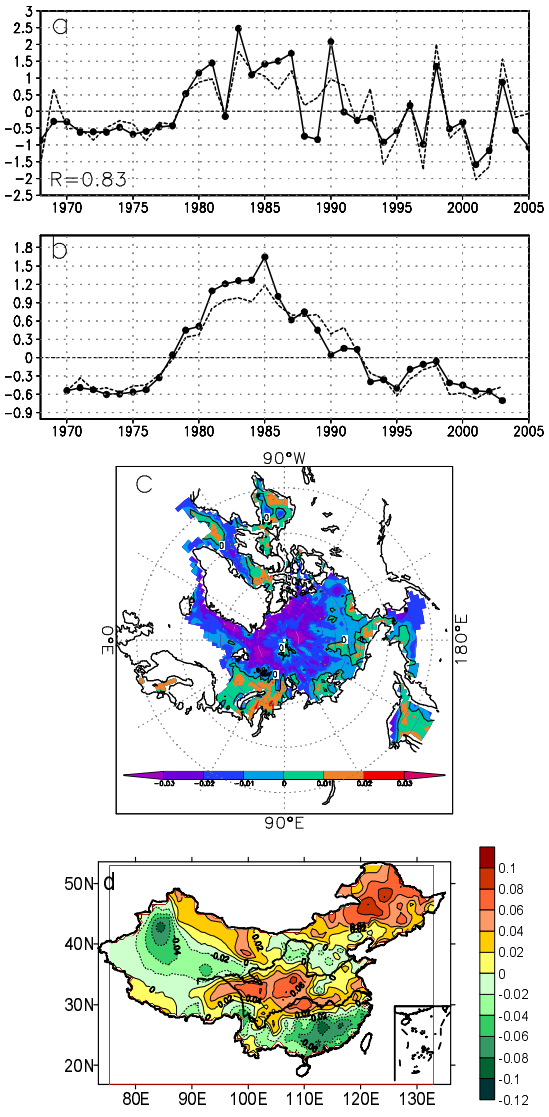

Fig. 1. (a) Normalized time series of spring SIC (solid line) and summer rainfall (dashed line) variations in the leading SVD mode, (b) same as in (a) but for their 5-year running mean, (c) spatial distribution of spring SIC variations in the leading SVD mode, (d) same as in (c) but for the summer rainfall variations. In (c) and (d), units are arbitrary (from Wu et al., 2009b).

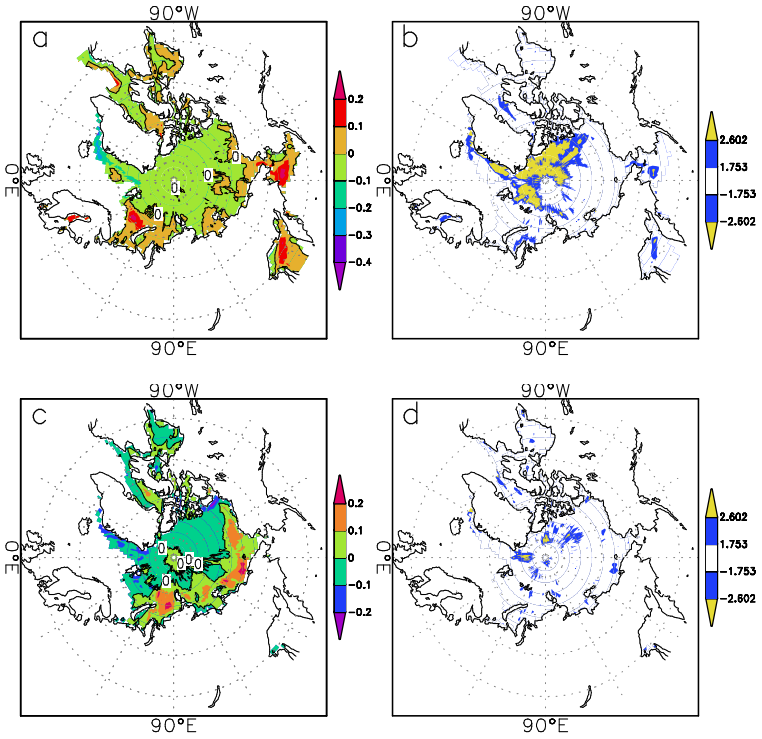

Fig. 2. (a) Differences in spring mean Arctic SIC between positive (1980, 1981, 1983, 1984, 1985, 1986, 1987, 1990, 1998, and 2003) and negative (1968, 1989, 1994, 1997, 2001, 2002, and 2005) phases, (b) statistical significance test for SIC differences, the shading area denotes the 0.05 and 0.01 significance levels, respectively, (c) and (d) respectively same as in (a) and (b) but for the summer season.

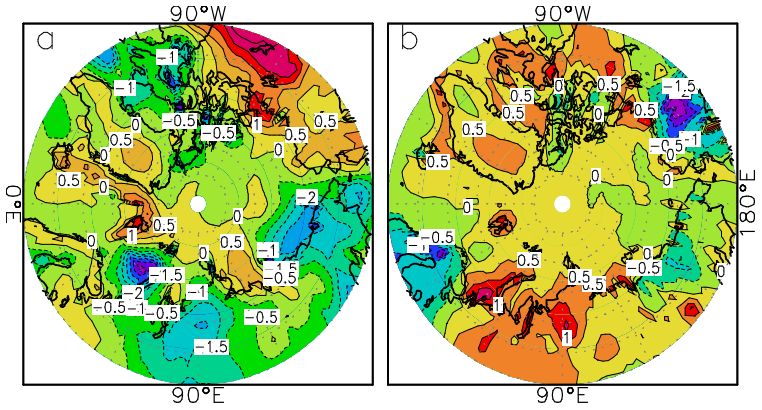

Fig. 3. Same as Figs. 2a and 2c but for surface air temperature, units: °C.

spatial distributions of the leading SVD between the spring Arctic SIC and summer rainfall in China, which accounts for 19% of the co-variance. Both Arctic SIC and summer rainfall in the leading SVD displayed a coherent interannual variability (the correlation between them is 0.83, Fig. 1a) and apparent interdecadal variations with phase changes occurring around 1978 and 1993 (Fig. 1b). The question is how to understand their possible linkage mechanisms. We performed a composite analysis based on the cases [the standard deviation of the spring SIC variability in the leading SVD>0.8 (1980, 1981, 1983, 1984, 1985, 1986, 1987, 1990, 1998, and 2003) and < -0.8 (1968, 1989, 1994, 1997, 2001, 2002, and 2005)]. Figures 2a and 2b show the spring SIC differences between the positive and negative phases and the statistical significance test. Significant decreases in spring SIC can be observed in the Arctic Ocean, the Greenland and the Beaufort

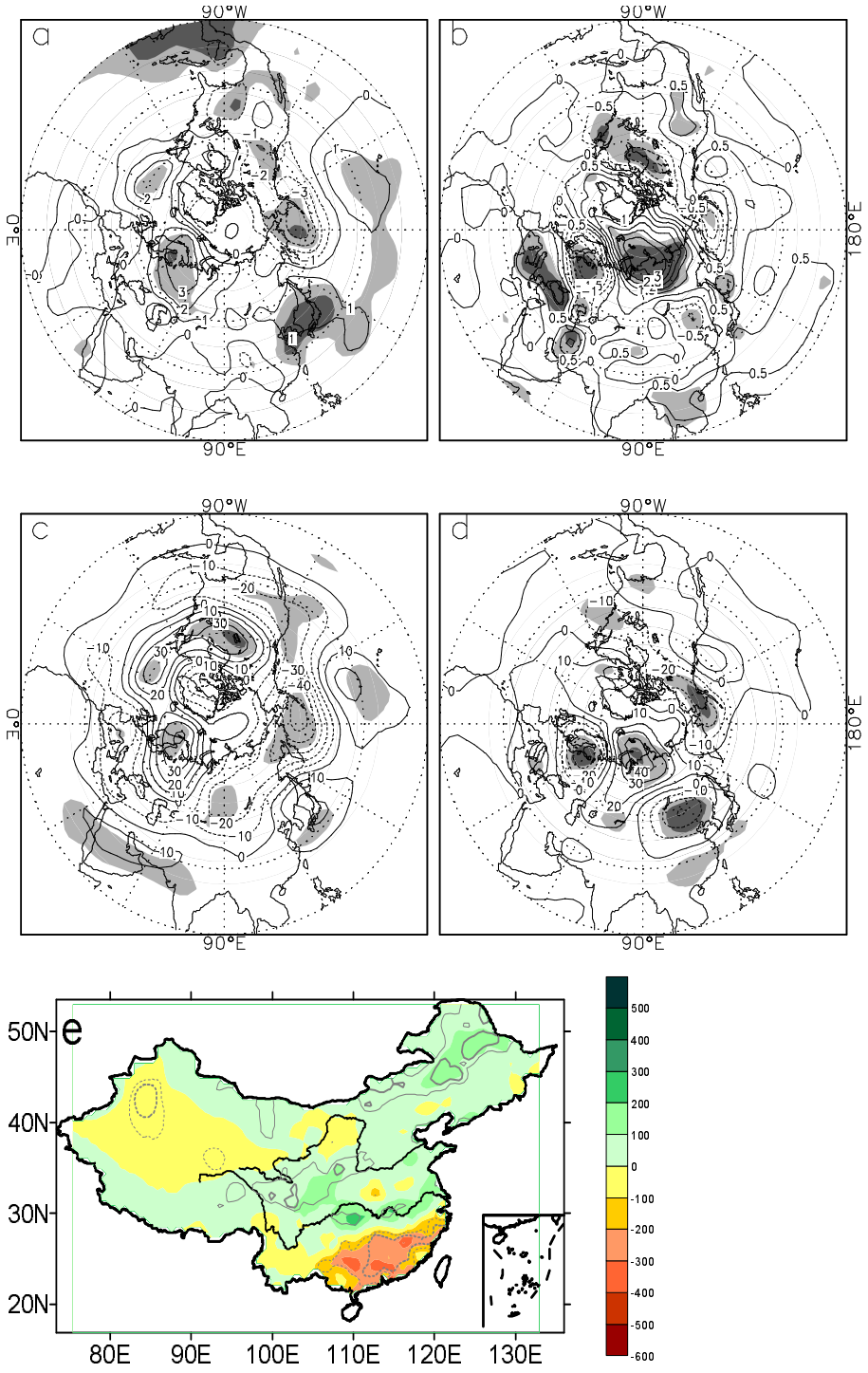

Fig. 4. (a) Spring and (b) summer SLP differences (units: hPa), the light and dark areas represent that the SLP differences exceed the 0.05 and 0.01 significance levels, respectively; (c) and (d) respectively same as in (a) and (b) but for the 500 hPa height differences (units: gpm); (e) summer rainfall differences (units: mm), the thin and thick lines denote that summer rainfall differences exceed the 0.05 and 0.01 significance levels, respectively. The cases for composite analysis are same as that in Fig. 2.

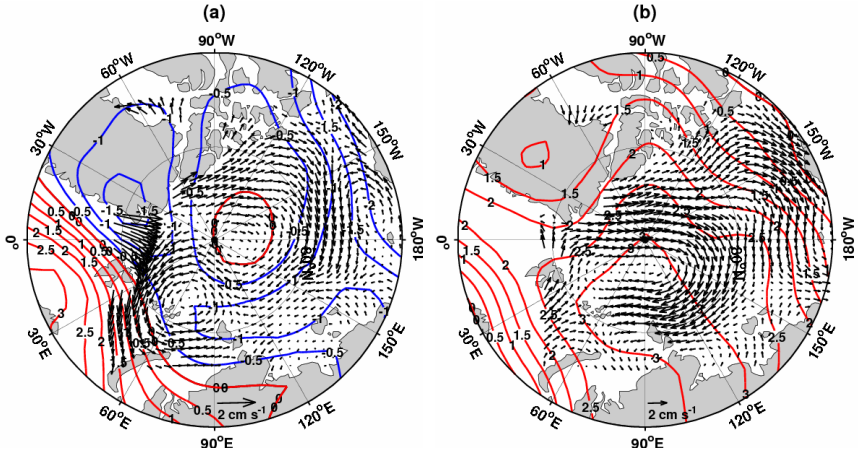

Fig. 5. Same as in Figs. 2a, and 2c, but for sea ice motion differences (units: cm). Contours are SLP differences (red: positive; blue: negative), and units are hPa.

Seas, whereas significant increases in SIC appear in the Kara, Bering, and Okhotsk Seas. During the following summer season, significant decreases in SIC still occur in the northern Greenland Sea and the Arctic Ocean, whereas SIC increases occur in the Siberian marginal seas (Figs. 2c and 2d). However, spring and summer SAT differences do not show coherent negative anomalies along the Siberian marginal seas (Fig. 3). This implies that SAT anomalies over the Siberian marginal seas cannot be explained by the local thermodynamics associated with the Arctic SIC variability. In fact, atmospheric forcing is a major reason for SIC anomalies, as many previous studies have indicated (Prinsenberg et al., 1997; Deser et al., 2000). During the spring season, significant positive SLP anomalies appear in East Asia and northern Europe (Fig. 4a). Negative SLP anomalies occupy most of the Arctic Ocean except the central Arctic basin where positive SLP anomalies are visible, leading to an anomalous anticyclonic sea ice motion pattern (Fig. 5a). It is seen that decreased sea ice export into the Greenland Sea and increased sea ice flow into the Barents Sea are in good agreement with the spatial distribution of spring SIC anomalies shown in Fig. 2a. Meanwhile, increased sea ice import from the western Arctic into the eastern Arctic is responsible for the decreased SIC shown in Fig. 2a. During the following summer, the center of the positive SLP anomalies from northern Europe move over the Kara and Laptev Seas, and positive SLP anomalies occupy near the entire Arctic Ocean (Fig. 4b). The strengthened SLP gradient leads to more sea ice export from the western Arctic into the eastern Arctic relative to the previous spring season (Fig. 5b and Fig. 2b) (Geostrophic winds account for more than 70% of the variance of the daily sea ice motion, Thorndike and Colony, 1982).

During the spring season, there are two opposite centers in the 500 hPa height anomalies, respectively, located over southwestern and northern Europe, and then they respectively move over northern Europe and the Kara Sea and anomalous amplitudes are significantly strengthened during the following summer (Figs. 4c and 4d). The spatial distribution of height anomalies shown in Fig. 4c closely resembles the Scandinavian pattern of Bueh and Nakamura (2007). During the summer season, negative SLP anomalies appear to the southeast of Lake Baikal and central China between the Yangtze River and the Yellow River (Fig. 4b). Corresponding 500 hPa height anomalies exhibit a wave train structure from northern Eurasia and the Siberian marginal seas extending southeastwards to northeast Asia, with significant negative anomalies over the southeast of Lake Baikal and significant positive anomalies over south and southeast China (Fig. 4d). Thus, the spatial distribution of SLP and 500 hPa height anomalies leads to more than normal summer rainfall in northeast China, between the Yangtze River and the Yellow River, and the Yangtze River (increased by 200 mm) and less rainfall in south and southeast China (decreased by 400 mm) (Fig. 4e).

4. Possible contributions from spring Arctic SIC to summer rainfall and circulation anomalies

The impacts of the East Asian summer monsoon on Chinese summer rainfall have been extensively explored (Tao and Chen, 1987; Wang et al., 2001; Ding and Chan, 2005; Ding et al., 2007; Wu et al., 2008). To evaluate the summer rainfall variance contributions derived from the EASM modes and the spring Arctic SIC sign, a linear regression of summer rainfall is performed, regression on the EASM modes and the spring Arctic SIC sign, respectively. We focus on the leading

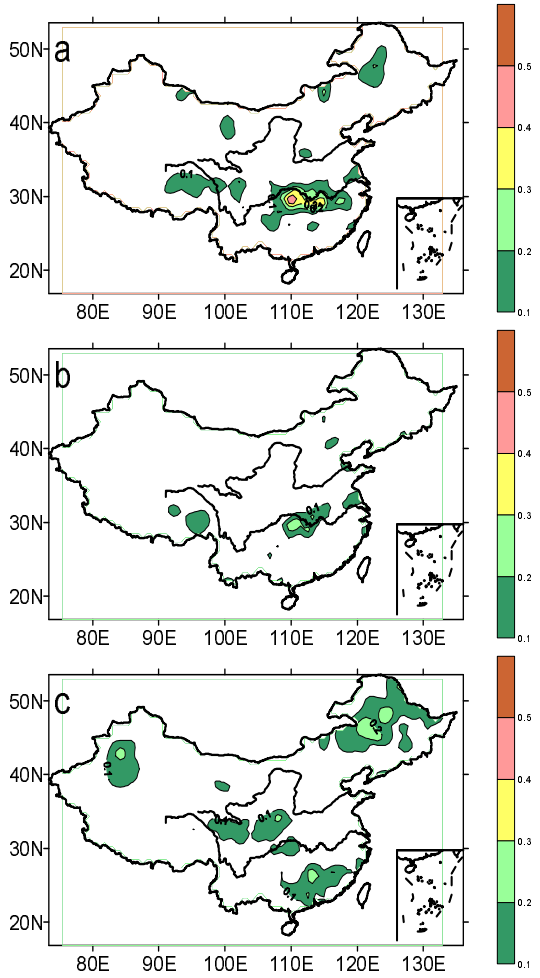

Fig. 6. Ratios of the accumulated variance of summer rainfall variability derived from (a) M11, (b) M12, (c) spring Arctic SIC sign in the leading SVD to the accumulated total variance of summer rainfall variability.

mode of the EASM variability, which is characterized by two distinct and alternating modes (M11 and M12) or their linear combination. Both of them correspond to the similar Pacific-Japan pattern in the 500 hPa height anomalies during the summer season (Wu et al., 2008). Contributions from the leading EASM modes are mainly confined to the Yangtze River valley (Figs. 6a and 6b), and M11 has the greatest contribution in the mid-low reaches of the Yangtze River valley (variance>30%). Contribution from the spring Arctic SIC sign is small in the Yangtze River valley; however, it is mainly in southern China, in between the Yangtze River and Yellow River, and northeast China, relative to the leading EASM mode (Fig. 6c).

Both the spring Arctic SIC and the Chinese summer rainfall show coherent interannual and interdecadal variations. Which time scale contributes more to the identified association? What are the features of the summer circulation anomalies on interannual and interdecadal time scales, respectively? To answer these questions, a linear regression on the spring SIC in the leading SVD is carried out on interdecadal and interannual time scales, respectively, and corresponding variance contributions also are calculated (Fig. 7). The results show that amplitudes of the interannual variability associated with the spring Arctic SIC are obviously greater relative to interdecadal variability (Figs. 7a and 7c), though they show a similar Eurasian wave train in the summer 500 hPa height anomalies. Over East Asia and the northern Asian continent, the variance contribution of the interannual variability is also greater relative to the interdecadal variability (Figs. 7b and 7d). Thus, it is expected that the association between the spring Arctic SIC and Chinese summer rainfall on interannual time scales is more important than that on interdecadal time scales, and Fig. 7e supports this speculation.

5. Another possible mechanism responsible for their linkage

In our previous study (Wu and Zhang, 2008), the summer Arctic dipole anomaly was identified, which is characterized by the second EOF of the summer (June–August) monthly mean SLP variability north of 70°N. In this section, an EOF analysis is applied to the summer mean SLP north of 70°N, averaged for three summer months (June–August). The motivation is to explore the linkage between the interannual variations of the summer Arctic dipole anomaly and the spring Arctic SIC/Chinese summer rainfall. For the reason we chosen such a domain for the EOF analyses, please refer to our previous studies (Wu et al., 2006; Wu and Johnson, 2007).

Figure 8 shows the spatial distribution and its time evolution of the second EOF of the summer mean SLP variability, accounting for 12.3% of the variance. According to North et al. (1982), the second EOF is well separated from the other EOFs. Compared to the Arctic dipole anomaly of the summer monthly mean SLP variability (Figs. 1, 2, and 6 of Wu and Zhang, 2008), the following differences are visible: (1) the negative center is located in the Beaufort Sea, and the "0"-isoline parallels the eastern Greenland coast (Fig. 8a). (2) Negative phases are frequent during the period of 1993 to 2001 (Fig. 8c) rather than the period of 1990 to 2004 in Wu and Zhang (2008). Thus, interdecadal variations in Fig. 8c are in agreement with that in Fig. 1c except for 2002–2003 where the dipole anomaly showed positive phases. The correlation between the dipole anomaly and the spring Arctic SIC in the leading SVD is 0.4 (at the marginal 0.01 significance level).

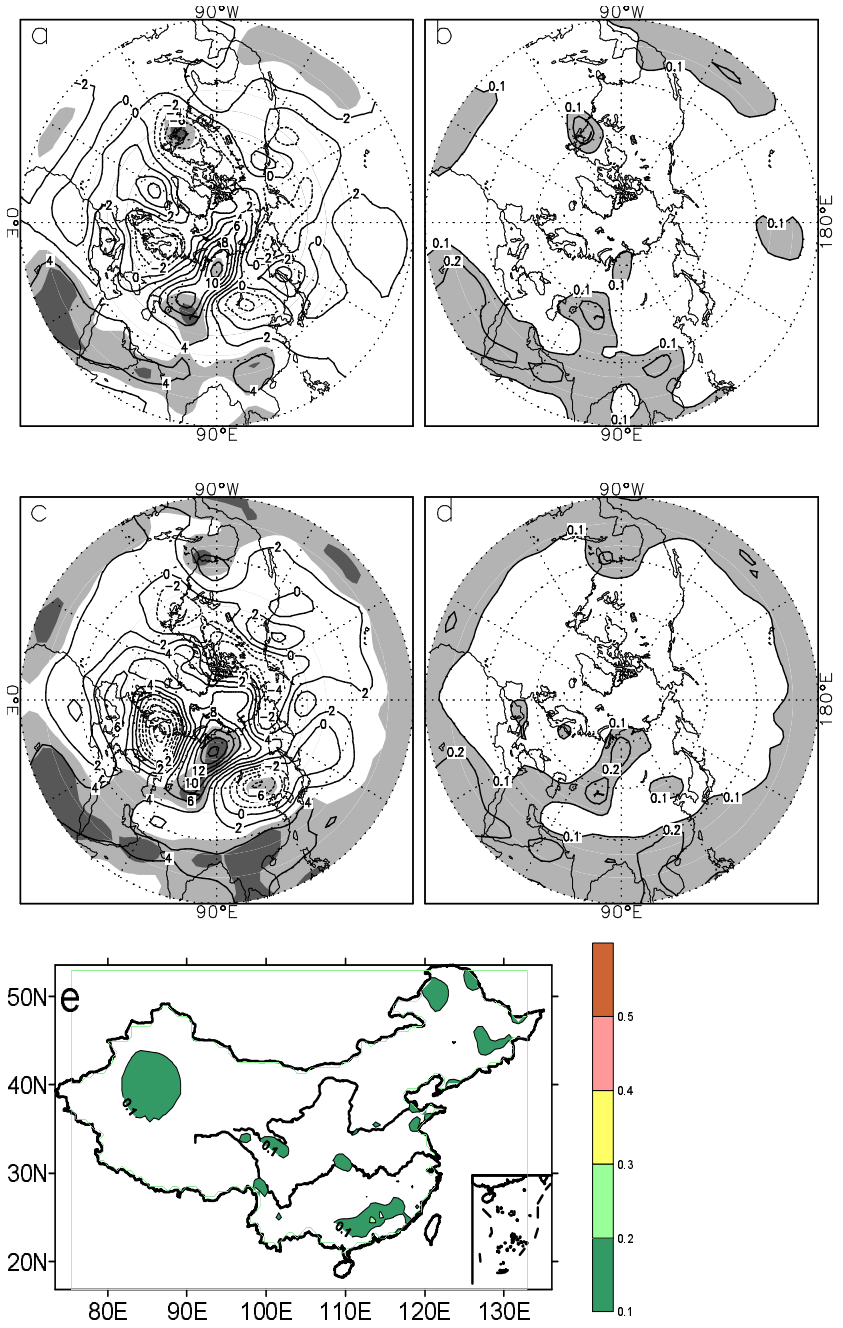

Fig. 7. (a) Summer 500 hPa height anomalies, derived from a linear regression on a 5-year running mean time series of spring SIC in the leading SVD during the period 1970–2003 (see Fig. 1b), (b) ratios of the accumulated variance of summer 500 hPa height variations induced by the spring SIC interdecadal variability to the accumulated total variance of 500 hPa height variability, (c) and (d) same as (a) and (b), respectively, but for spring SIC interannual variability during the period 1970–2003, (e) same as (b) but for Chinese summer rainfall. In (a) and (c), the shading areas denotes 500 hPa height anomalies exceeding the 0.05 and 0.01 significance levels, respectively. In (b) and (d), the shading areas represent the variance contribution$\geqslant$0.1.

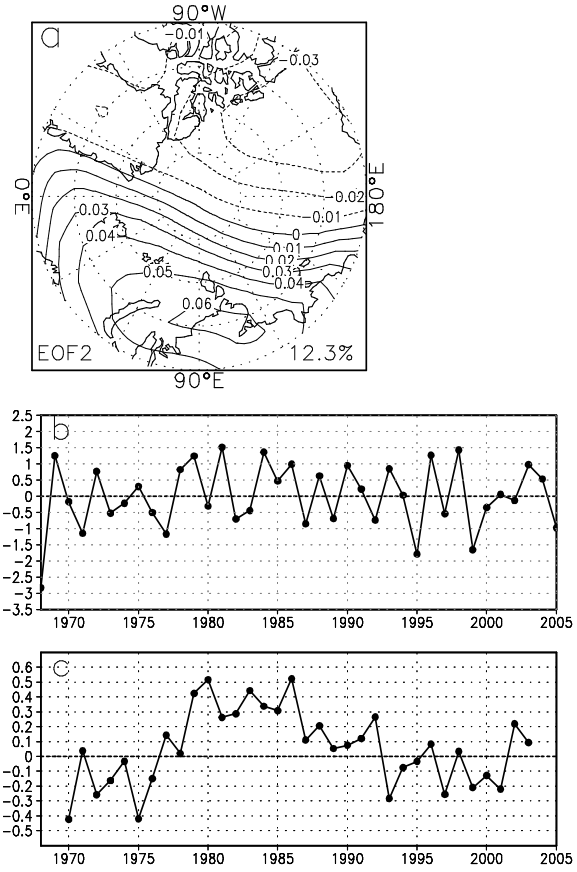

Fig. 8. (a) The spatial distribution and (b) normalized time series of the second EOF of the summer mean SLP variability north of 70°N, accounting for 12.3% of the variance, (c) a 5-year running mean of (b).

The 500 hPa height difference between the positive (σ >0.8: 1969, 1978, 1979, 1981, 1984, 1986, 1990, 1993, 1996, 1998, and 2003) and the negative (σ < −0.8: 1968, 1971, 1977, 1987, 1995, 1999, and 2005) phases of the dipole anomaly show apparent evolution characters from spring to summer (Fig. 9). It is seen that the positive anomalous center over northern Europe during spring moves to the Barents and the Kara Seas during the following summer, and the negative anomalous center from northern Asia moves to the southeast of Lake Baikal region. Spring and summer 500 hPa height anomalies show an opposite scenario over East Asia north of 40°N, the Arctic region, and southwest of the Bering Sea.

Compared to the negative phases of the dipole anomaly, the positive phases correspond to decreased spring SIC in most of the Arctic Ocean and the Greenland Sea and increased SIC in the Barents, Kara, and Laptev Seas (Figs. 10a and 10b). During the ensuing summer, decreased SIC in the Greenland Sea and most of the Arctic Ocean and increased SIC in most of the Siberian marginal seas are concurrent (Figs. 10c and 10d). The spatial distribution of summer SIC anomalies in Fig. 10c is dynamically consistent with the SLP anomalies in Fig. 8a. Figure 10 shows a great similarity to Fig. 2 except for the Bering Sea and the Okhotsk Sea where the differences in the spring SIC are robust. Decreased spring SIC in most of the Arctic Ocean leads to increased heat fluxes from the ocean into the atmosphere, near-surface warming, and below normal SLP. On the contrary, increased spring SIC in the Barents, Kara, and Laptev Seas may induce the local positive SLP anomalies (Wu et al., 2004). Thus, the spatial distribution of spring SIC anomalies provides an important external forcing for the summer dipole anomaly. Simulation results also suggest that enhanced surface heat flux anomalies derived from the Arctic SIC simulations may preferentially excite internal modes of atmospheric variability (Alexander et al., 2004).

The spatial distribution of the correlations between the summer dipole anomaly and Chinese summer rainfall shows significant positive correlations in northeast China and significant negative correlations in south and southeast China (Fig. 11a), consistent with the composite analysis of summer rainfall shown in Fig. 4e. The correlation between the dipole anomaly and the Chinese summer rainfall variations in the leading SVD is 0.51 (at the 0.01 significance level). Consequently, the summer dipole anomaly may be another mechanism responsible for the linkage between the spring Arctic SIC and Chinese summer rainfall. Although the atmospheric forcing may explain Arctic SIC variability from spring to summer the feedback of Arctic SIC anomalies on the atmosphere may modify the central location, intensity, and periodicity of the summer dipole anomaly, particularly on interdecadal time scales (Fig. 8c). Compared to the summer Arctic dipole anomaly, the relationship between the AO and the Chinese summer rainfall variability is weak, as shown in Figs. 11b, 11c. A significant negative correlation between the spring (March–May) AO and Chinese summer rainfall appears in the mid-low reaches of the Yangtze River valley (Fig. 11b). Gong et al. (2002) also suggested that the AO in May is significantly correlated to the filtered summer rainfall in the mid-low reaches of the Yangtze River valley. Significant positive correlations between the summer AO and Chinese summer rainfall can be observed in the Yellow River valley (Fig. 11c).

6. Discussions

On interdecadal time scales, a coherent negative phase of spring SIC variability can be observed after

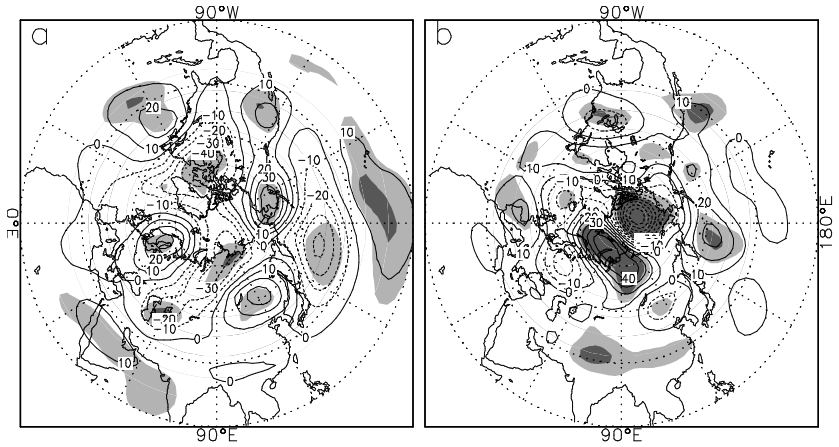

Fig. 9. (a) Spring and (b) summer mean 500 hPa height differences between the positive (σ >0.8: 1969, 1978, 1979, 1981, 1984, 1986, 1990, 1993, 1996, 1998, and 2003) and negative phases ($\sigma < -0.8$: 1968, 1971, 1977, 1987, 1995, 1999, and 2005) of the summer dipole anomaly, units are gpm. The shading area denotes that the 500 hPa height differences exceed the 0.05 and 0.01 significance level, respectively.

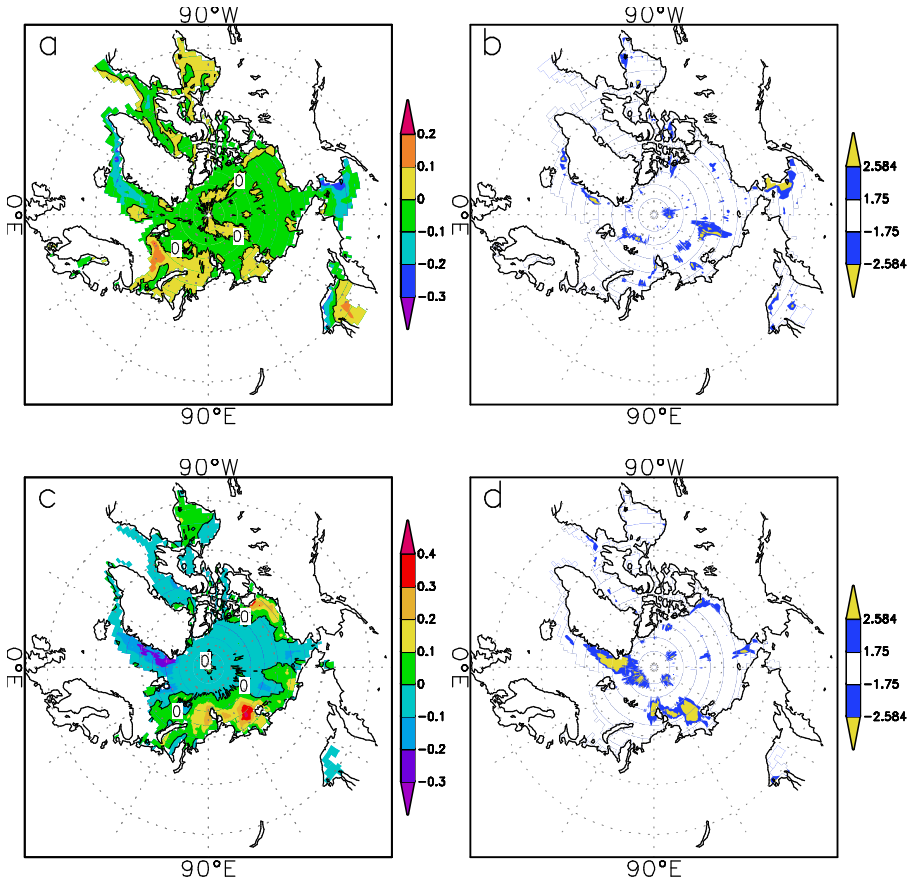

Fig. 10. (a) Differences in spring mean Arctic SIC between positive and negative phases of the summer dipole anomaly, (b) statistical significance test for SIC differences, the shading area denotes the 0.05 and 0.01 significance levels, respectively, (c) and (d) respectively same as in (a) and (b) but for the summer season. The cases for composite analysis are the same as that in Fig. 9.

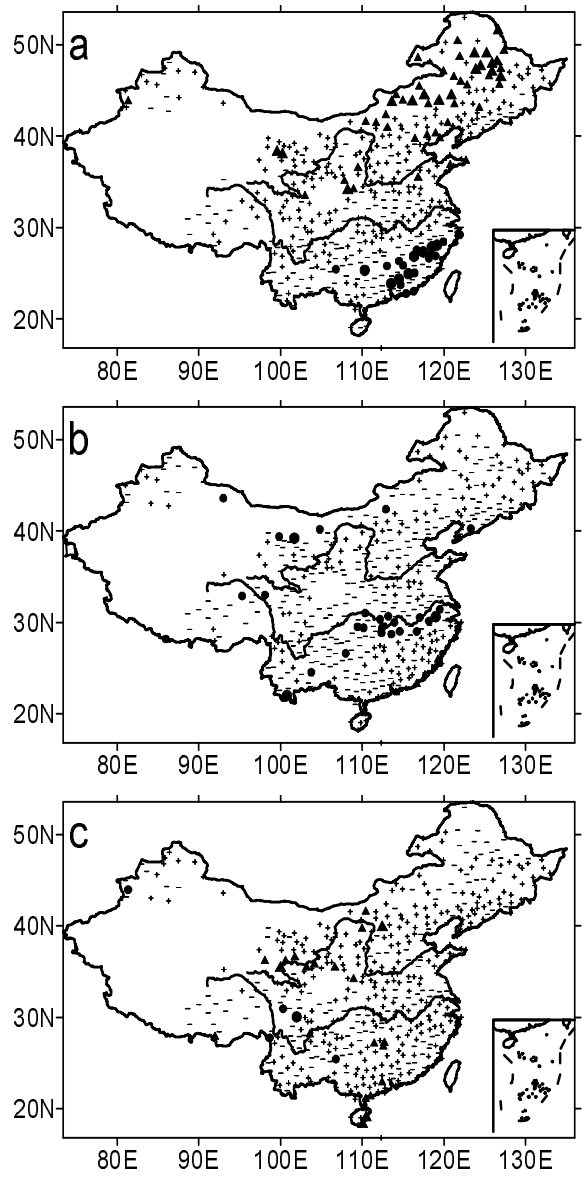

Fig. 11. The spatial distribution of correlations (+: positive correlation; −: negative correlation) between Chinese summer station rainfall and (a) the summer dipole anomaly, (b) the spring AO, and (c) the summer AO. The triangle (dot) denotes significant positive (negative) correlation [above the 0.05 and 0.01 (bigger symbol) significance levels].

1992 (Fig. 1b). Correspondingly, positive 500 hPa height anomalies frequently occupy northeast Asia (not shown). Thus, summer rainfall frequently shows a positive anomaly in south and southeast China and a negative anomaly in northeast China (Fig. 1d), consistent with interdecadal variations of the Chinese summer rainfall in Ding et al. (2007, see their Fig. 2). Sun and Chen (2003) indicated that in addition to interdecadal variations in the Chinese summer rainfall, positive 500 hPa height anomalies over the mid-high latitudes of East Asia may be one of the reasons for persistent droughts in north and northeast China. However, the leading mode of the EASM variability cannot explain the interdecadal summer rainfall variations that occurred since the early 1990s because the EASM mode was strengthened over southern China during the late 1980s to the late 1990s (Wu et al., 2008, see their Figs. 1 and 2). Thus, we speculate that anomalous external forcing, such as Eurasian snow cover and Arctic sea ice, and atmospheric teleconnection patterns in the northern high latitudes may be reasons responsible for severe droughts in north and northeast China and much more significant rainfall in south and southeast China in recent decades.

Although the evolution of atmospheric circulation anomalies from spring to summer may explain Arctic SIC and Chinese summer rainfall variations, some important issues still remain unclear. For example, what process controls the evolution of atmospheric circulation anomalies from spring to summer, and what is the reason for spring atmospheric circulation anomalies over the Europe sector, and why spring atmospheric circulation anomalies exhibit a quasi-barotropic structure over Europe and a baroclinic structure over the northern Asian continent (Fig. 4). Additionally, as indicated in the introduction, sea ice variation can influence the atmosphere, however, this study does not explore how the spring SIC variation affects the atmosphere; whether ENSO events play a role in their association? These unclear issues need to be investigated in the future.

7. Conclusions

The analysis results suggest that the evolution of atmospheric circulation anomalies from spring to summer, to a great extent, may explain the fact that the spatial distributions of the spring and summer Arctic SIC anomalies and summer atmospheric circulation anomalies are dynamically consistent with the Chinese summer rainfall anomalies. Corresponding to the spring negative SIC anomalies in the Greenland Sea and the western Arctic Ocean, a simultaneous wave train in the 500 hPa height anomalies appears over Eurasia with three anomalous centers located respectively over southwestern Europe (negative center), northern Europe (positive center), and west of the Lake Baikal region (negative center). From spring to summer, the three anomalous centers move to, respectively, northern Europe, the Kara Sea, and southeast of Lake Baikal-northeast China. The summer wave train is believed to contribute to the increased summer rainfall in (a) north and northeast China, (b)

central China between the Yangtze River and the Yellow River, and (c) the regions along the Yangtze River, and the decreased summer rainfall in South and Southeast China. Although spring Arctic SIC and Chinese summer rainfall exhibit coherent interannual and interdecadal variations, their association on interannual time scales is more important relative to that on interdecadal time scales.

The summer Arctic dipole anomaly, characterized by the second EOF of the summer mean SLP variability north of 70°N, may serve as the bridge linking spring Arctic SIC and Chinese summer rainfall, and its interdecadal variation may reflect the feedback of Arctic SIC on the atmosphere. The summer Arctic dipole anomaly shows a closer relationship with the Chinese summer rainfall relative to the AO.

Acknowledgements. Authors thank NCEP and NCAR, the British Atmospheric Data Centre, and the National Meteorological Information Centre of China for respectively providing reanalysis datasets, SIC data, and station rainfall data. This study was supported by the National Key Basic Research and Development Project of China (Grant Nos. 2004CB418300 and 2007CB411505), Chinese COPES project (GYHY200706005), and the National Natural Science Foundation of China (Grant No. 40875052).

REFERENCES

Aagaard, K., and E. C. Carmack, 1989: The role of sea ice and other freshwater in the Arctic circulation. *J. Geophys. Res.*, **94**, 305–311.

Alexander, M. A., and Coauthors, 2004: The atmospheric response to realistic sea ice anomalies in an AGCM during winter. *J. Climate*, **17**, 890–905.

Bueh, C., and H. Nakamura, 2007: Scandinavian pattern and its climate impact. *Quart. J. Roy. Meteor. Soc.*, **133**, 2117–2131.

Cavalieri, D. J., and C. L. Parkinson, 1987: On the relationship between atmospheric circulation and fluctuations in sea ice extents of the Bering and Okhotsk Seas. *J. Geophys. Res.*, **92**, 7141–7162.

Chang, C.-P., Y. Zhang, and T. Li, 2000: Interannual and interdecadal variations of the East Asian summer monsoon and tropical Pacific SSTs. Part I: Roles of the subtropical ridge. *J. Climate*, **13**, 4310–4325.

Deser, C., and M. L. Blackmon, 1993: Surface climate variations over the North Atlantic Ocean during winter: 1900–1989. *J. Climate*, **6**, 1743–1754.

Deser, C., G. Magnusdottir, R. Saravanan, and A. Phillips, 2004: The effects of North Atlantic SST and sea ice anomalies on the winter circulation in CCM3. Part II: Direct and indirect components of the response. *J. Climate*, **17**, 877–889.

Deser, C., J. E. Walsh, and M. S. Timlin, 2000: Arctic sea ice variability in the context of recent atmospheric circulation trends. *J. Climate*, **13**, 617–633.

Ding, Y., and J. Chan, 2005: The East Asian summer monsoon: An overview. *Meteor. Atmos. Phys.*, **89**, 117–142.

Ding, Y., Z. Wang, and Y. Sun, 2007: Inter-decadal variation of the summer precipitation in East China and its association with decreased Asian summer monsoon. Part I: Observational evidences. *International Journal of Climatology*, **28**, doi: 10.1002/joc.1615.

Fang, Z., and J. M. Wallace, 1994: Arctic sea ice variability on a timescale of weeks: Its relation to atmospheric forcing. *J. Climate*, **7**, 1897–1913.

Gong, D. Y., J. H. Zhu, and S. W. Wang, 2002: Significant correlation between spring AO and summer rainfall in the Yangtze River valley. *Chinese Science Bulletin*, **47**, 546–549. (in Chinese)

Honda, M., K. Yamazaki, Y. Tachibana, and K. Takeuchi, 1996: Influence of Okhotsk sea-ice extent on atmospheric circulation. *Geophys. Res. Lett.*, **23**, 3595–3598.

Hu, Z. Z., 1997: Inter-decadal variability of summer climate over East Asia and its association with 500 hPa height and global sea surface temperature. *J. Geophys. Res.*, **102**, 19403–19412.

Ju, J. H., and J. Slingo, 1995: The Asian summer monsoon and ENSO. *Quart. J. Roy. Meteor. Soc.*, **121**, 1133–1168.

Lazier, J., 1988: Temperature and salinity changes in the deep Labrador Sea 1962–1986. *Deep-Sea Res.*, **35**, 1247–1253.

Lenderink, G., and R. J. Haarsma, 1996: Modeling convective transitions in the presence of sea ice. *J. Phys. Oceanogr.*, **26**, 1448–1467.

Li, T., and B. Wang, 2005: A review on the western North Pacific monsoon: Synoptic-to-interannual variabilities. *Terrestrial, Atmospheric and Oceanic Sciences*, **16**, 285–314.

Magnusdottir, G., C. Deser, and R. Saravanan, 2004: The effects of North Atlantic SST and sea ice anomalies on the winter circulation in CCM3. Part I: Main features and storm track characteristics of the response. *J. Climate*, **17**, 857–876.

Mauritzen, C., and S. Häkkinen, 1997: Influence of sea ice on the thermohaline circulation in the Arctic-North Atlantic Ocean. *Geophys. Res. Lett.*, **24**, 3257–3260.

Mysak, L. A., and S. A. Venegas, 1998: Decadal climate oscillation in the Arctic: A new feedback loop for atmosphere-ice-ocean interactions. *Geophys. Res. Lett.*, **25**, 3607–3610.

Mysak, L. A., D. K. Manak, and R. F. Marsden, 1990: Sea-ice anomalies observed in the Greenland and Labrador Seas during 1901-1984 and their relation to an interdecadal Arctic climate cycle. *Climate Dyn.*, **5**, 111–133.

Niu, T., P. Zhao, and L. Chen, 2003: Effects of the sea-ice along the North Pacific on summer rainfall in China. *Acta Meteorologica Sinica*, **17**, 52–64.

North, G. R., T. L. Bell, R. F. Cahalan, and F. J. Moeng, 1982: Sampling errors in the estimation of EOFs.

Mon. Wea. Rev., **110**, 699–706.

Prinsenberg, S. J., I. K. Peterson, S. Narayanan, and J. U. Umoh, 1997: Interaction between atmosphere, ice cover, and ocean off Labrador and Newfoundland from 1962–1992. *Canadian Journal of Fisheries and Aquatic Sciences*, **54**, 30–39.

Rigor, I. G., J. M. Wallace, and R. L. Colony, 2002: Response of sea ice to the Arctic Oscillation. *J. Climate*, **15**, 2648–2663.

Sun, L. H., and X. F. Chen, 2003: Decade climate characters and formation condition of flooding in south China and drought in north China. *J. Appl. Meteor. Sci.*, **14**, 641–647.

Tao, S., and L. Chen, 1987: A review of recent research on the East Asian summer monsoon in China. *Monsoon Meteorology*, C.-P. Chang and T. N. Krishnamurti, Eds., Oxford University Press, 60–92.

Thorndike, A. S., and R. Colony, 1982: Sea ice motion in response to geostrophic winds. *J. Geophys. Res.*, **87**, 5845–5852.

Vinje, T., 2001: Fram Strait ice fluxes and atmospheric circulation: 1950–2000. *J. Climate*, **14**, 3508–3517.

Wang, B., and T. Li, 2004: East Asian monsoon and ENSO interaction. *East Asian Monsoon*. World Scientific Publishing Company, C. P. Chang, Ed., 177–212.

Wang, B., R. Wu, and X. Fu, 2000: Pacific-East Asian teleconnection: How does ENSO affect East Asian climate? *J. Climate*, **13**, 1517–1536.

Wang, B., R. Wu, and K. Lau, 2001: Interannual variability of the Asian summer monsoon: Contrasts between the Indian and the western North Pacific-East Asian monsoon. *J. Climate*, **14**, 4073–4090.

Wang, B., R. Wu, and T. Li, 2003: Atmosphere-warm Ocean interaction and its impact on Asian-Australian monsoon variation. *J. Climate*, **16**, 1195–1211.

Wang, B., I. S. Kang, and J. Y. Lee, 2004: Ensemble simulations of Asian-Australian monsoon variability by 11 AGCMs. *J. Climate*, **17**, 803–818.

Wang, B., Q. Ding, X. Fu, I. Kang, K. Jin, and J. Shukla, 2005: Fundamental challenge in simulation and precipitation of summer monsoon rainfall. *Geophys. Res. Lett.*, **32**, L15711, doi: 10.1029/2005GL022734.

Walsh, J. E., 1983: Role of sea ice in climate variability: Theories and evidence. *Atmos.-Ocean*, **21**, 229–242.

Weng, H., K.-M. Lau, and Y. Xue, 1999: Multi-scale summer rainfall variability over China and its long-term link to global sea surface temperature variability. *J. Meteor. Soc. Japan*, **77**, 845–857.

Wu, B., and M. A. Johnson, 2007: A seesaw structure in SLP anomalies between the Beaufort Sea and the Barents Sea. *Geophys. Res. Lett.*, **34**, L05811, doi: 10.1029/2006GL028333.

Wu, B., and R. Zhang, 2008: Arctic dipole anomaly and summer rainfall in northeast China. *Chinese Science Bulletin*, **53**, 2222–2229.

Wu, B., J. Wang, and J. Walsh, 2004: Possible feedback of winter sea ice in the Greenland and the Barents Sea on the local atmosphere. *Mon. Wea. Rev.*, **132**, 1968–1876.

Wu, B., J. Wang, and J. Walsh, 2006: Dipole anomaly in the winter arctic atmosphere and its association with sea ice motion. *J. Climate*, **19**, 210–225.

Wu, B., R. Zhang, Y. Ding, and R. D'Arrigo, 2008: Distinct modes of the East Asian summer monsoon. *J. Climate*, **21**, 1122–1138.

Wu, B., K. Yang, and R. Zhang, 2009a: Eurasian snow cover variability and its association with summer rainfall in China. *Adv. Atmos. Sci.*, **26**(1), 31-44, doi: 10.1007/s00376-009-0031-2.

Wu, B., R. Zhang, B. Wang, and R. D'Arrigo, 2009b: On the association between spring Arctic sea ice concentration and Chinese summer rainfall. *Geophys. Res. Lett.*, **36**, L09501, doi:10.1029/2009GL037299.

Wu, R., and B. P. Kirtman, 2007: Observed relationship of spring and summer East Asian rainfall with winter and spring Eurasian snow. *J. Climate*, **20**, 1285–1304.

Yang, F., and K.-M., Lau, 2004: Trend and variability of China precipitation in spring and summer: Linkage to sea-surface temperature. *International Journal of Climatology*, **24**, 1625–1644.

Yang, S., and L. Xu, 1994: Linkage between Eurasian winter snow cover and regional Chinese summer rainfall. *International Journal of Climatology*, **11**, 3230–3246.

Yang, S., K.-M. Lau, and K. M. Kim, 2002: Variations of the East Asian jet stream and Asian-Pacific-American winter climate anomalies. *J. Climate*, **15**, 306–325.

Zhang, R., A. Sumi, and M. Kimoto, 1996: Impact of El Niño on the East Asian monsoon: A diagnostic study of the '86/87 and '91/92 events. *J. Meteor. Soc. Japan*, **74**, 49–62.

Zhang, R., A. Sumi, and M. Kimoto, 1999: A diagnostic study of the impacts of El Niño on the precipitation in China. *Adv. Atmos. Sci.*, **16**, 229–241.

Zhao, P., X. D. Zhang, X. J. Zhou, M. Ikeda, and Y. H. Yin, 2004: The sea ice extent anomaly in the North Pacific and its impact on the east Asian summer monsoon rainfall. *J. Climate*, **17**, 3434–3447.